Preparation of BN Microtubes/Nanotubes with a Unique Chemical Process

ARTICLE *in* THE JOURNAL OF PHYSICAL CHEMISTRY C · FEBRUARY 2008

Impact Factor: 4.77 · DOI: 10.1021/jp804286x · Source: OAI

6 AUTHORS, INCLUDING:

Mikhael Bechelany
Université de Montpellier
113 PUBLICATIONS **1,349** CITATIONS
SEE PROFILE

Arnaud Brioude
Claude Bernard University Lyon 1
108 PUBLICATIONS **1,962** CITATIONS
SEE PROFILE

Samuel Bernard
Université de Montpellier
106 PUBLICATIONS **1,244** CITATIONS
SEE PROFILE

Philippe Miele
Ecole Nationale Supérieure de Chimie de…
292 PUBLICATIONS **4,390** CITATIONS
SEE PROFILE

Preparation of BN Microtubes/Nanotubes with a Unique Chemical Process

Mikhael Bechelany,[†] Arnaud Brioude,[†] Pierre Stadelmann,[‡] Samuel Bernard,[†] David Cornu,[†,*] and Philippe Miele[†]

Laboratoire des Multimatériaux et Interfaces, UMR 5615, CNRS, Université de Lyon, Université Lyon 1, 43 bd du 11 nov. 1918, F-69622 Villeurbanne, France, and Interdepartmental Center of Electron Microscopy, Swiss Federal Institute of Technology (EPFL), bat. MX-C 134, CH-1015, Lausanne, Switzerland

Received: May 14, 2008; Revised Manuscript Received: September 15, 2008

BN tubular micro-/nanostructures were prepared in large scale from a simple unique chemical process onto the surface of a graphite substrate, using polypropylene and boron oxide as solid sources, and under an ammonia flow. The as-grown product is featured by a unique hierarchical tubular structure with BN microtubes covered by BN multiwall nanotubes a few nanometers in diameters. Elegant BN flowers were grown on the same substrate when omitting carbon precursors. These BN micro-/nanotubes open new perspectives in (nano)-composite materials with enhanced matrice-to-fibers bonding.

Introduction

In the past decade, considerable effort has been devoted to the synthesis and characterization of boron nitride single- and multiwall nanotubes (BN NTs). Both theoretical predictions and experimental investigations highlight their unique chemical and physical properties.[1,2] These features yield these 1D nanostructures, and their derivatives like carbon-doped BN NTs, to find various potential/demonstrated applications in a wide range of domains going from composite materials, to gas storage systems, to optoelectronic devices. Concerning the fabrication of BN NTs, various approaches have been investigated. They were first prepared by Chopra et al. by arc-discharge between BN-filled tungsten electrodes.[3] This method was subsequently improved by other groups.[4] Laser ablation,[5] plasma-based techniques,[6] carbo-[7] and amino-[8] thermal reduction route, high-pressure techniques,[9] and the template-assisted process[10] have also been developed. The ball milling technique was demonstrated to be a convenient way to produce bamboo-like BN nanotubes in high yield.[11] Velazquez-Salazar et al. have suggested that metallic nanoparticules may play a key role in the involved growth mechanism (root growth process).[12] Finally and in parallel with pending works on carbon NTs, the chemical vapor deposition (CVD) route is extensively studied. Lourie et al. have prepared BN NTs from a molecular precursor, the borazine [$H_3B_3N_3H_3$], and nickel boride particles.[13] Moreover various nanosized particles can be used to promote the growth of BN NTs or nanowires. Among the latter the techniques developed by Bando's group appear as the most valuable. First they established that BN NTs can be prepared from BNO nanoclusters using $B_4N_3O_2H$ as precursor.[14] This technique gives BN NTs with high chemical purity but they have reported yields too low for industrial applications (2 mg from 2 g of $B_4N_3O_2H$). This drawback has been overcome by the same group in 2002 with the large-scale production of BN NTs from B and MgO mixture.[15] However, the elimination of the byproduct, Mg, by evaporation is not so simple, leading to the presence of residual Mg in the sample. This technique was subsequently improved in 2005 by the use of a mixture of MgO and FeO to promote the growth.[16] However, for some selected applications and/or for some experimental investigations of the physical properties of BN NTs, the presence of residual Mg and/or Fe may be a crucial problem. More recently our group has demonstrated that a chemical route using liquid polymeric precursor can be used to prepared BN polycrystalline and multiwall nanotubes.[17] The synthesis, characterization, properties, and potential applications of BN nanotubes are fully described in two recent reviews.[18,19] The authors highlight a relatively small number of papers devoted to BN NTs, in respect to their fundamental interests and potential applications, attributed to significant difficulties in their preparation compared to those of carbon analogues. We present here a simple, cheap, and high-yield route to unique BN micro-/nanotubes. Our strategy is based on nonsensitive cheap reagents, rather than air-sensitive liquid precursors which require specific equipment like a glovebox or vacuum/argon lines. We have to mention that the present process is based on a method we developed for growing silicon carbide (SiC) nanowires onto the surface of a graphite condensation plate and from in situ generated volatile precursors.[20]

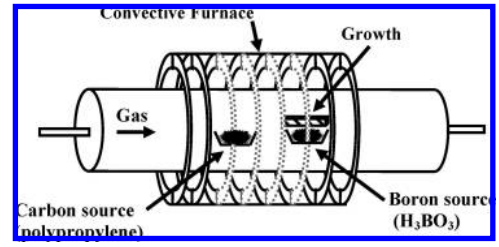

Figure 1. Experimental setup used for the fabrication of BN micro-/nanotubes and flowers.

Experimental Section

The experiments were conducted according to the experimental setup schematically represented in Figure 1. This setup consisted of an alumina boat containing a carbon source (6 g of polypropylene (Aldrich, purum)), followed by a second alumina boat containing a boron source (2 g of boron oxide, B_2O_3, prepared by deshydratation of a boric acid powder (Aldrich, purum)), which was partially covered by a graphite

* Corresponding author. E-mail: david.cornu@univ-lyon1.fr.
† Université Lyon 1.
‡ Swiss Federal Institute of Technology.

10.1021/jp804286x CCC: $40.75
Published on Web 11/01/2008

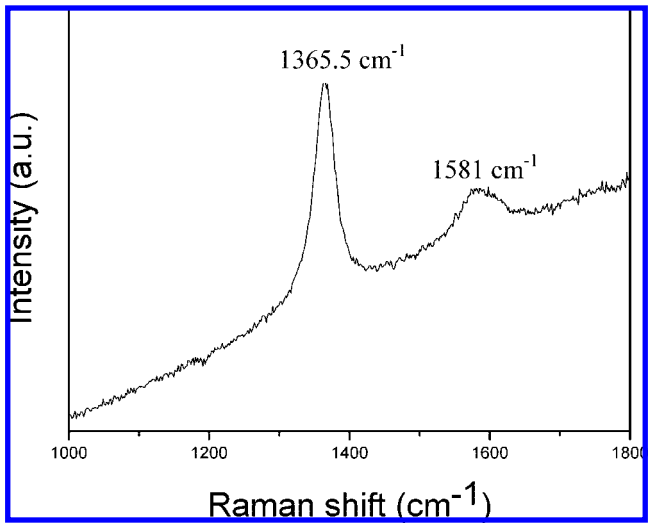

Figure 2. Raman spectrum of the as-grown product obtained by using a graphite condensation plate.

condensation plate (growth support). The latter was carved in a commercial anisotropic graphite block (Carbone Lorraine C2120) so that the condensation plate will not hermetically close the alumina boat. The entire setup was placed into the hot-zone of the alumina tube of a convective furnace equipped with two water-cooled flasks at each end. All of the experiments were conducted under ammonia, which is supposed to act as a reactive flowing gas, at a very low flow rate (10 mL·min^{-1}), heated to 1500 °C (400 deg·h^{-1}), and maintained at this temperature for 10 h before cooling to room temperature (400 deg·h^{-1}). XRD analyses were performed with a Philipps PW 3040/60 X'Pert PRO X-ray diffraction system operating at 30 mA and 40 kV. A Hitachi Model S800 was used for SEM measurements. TEM (TOPCON 002B) and EELS (LGatan PEELS model 666) studies were conducted to determine the chemical composition and the structural characteristics of the as-grown nanostructures.

Results and Discussion

Synthesis and Characterization of BN Tubular Structures with Hierarchical Cavity Sizes. When a piece of graphite is used to cover the alumina boat containing the boron source, a mass of ~100 mg of a light-gray solid is collected at the lower face of this condensation plate. XRD diffraction performed on the as-obtained product revealed that it is composed of the hexagonal polytype of boron nitride, *h*-BN. This result was confirmed by micro-Raman spectroscopy (Figure 2). The Raman spectrum of the product shows two peaks. The first one at 1365.5 cm^{-1} (FHWM 32 cm^{-1}), was attributed to the E_{2g} vibration mode of *h*-BN. This mode is located at 1368 cm^{-1} in polycrystalline *h*-BN powder.[21] The FHWM value is close to the one given in the literature for BN NTs[22] and significantly higher than the one reported for micrometric powders (13 cm^{-1}). This difference is not surprising since the interplanar distances in BN NTs are higher than that in *h*-BN. It is interesting to notice than the peak centered at 1581 cm^{-1} shows the presence of carbon[23] in the as-grown product, in good agreement with its light-gray coloration.

SEM investigation of the sample has revealed a unique tubular morphology with hierarchical cavity sizes: microtubes 1−20 μm in diameter (Figure 3a) which are entirely covered by a high density of nanotubes (Figure 3b). The nanotubes are very long (~0.5 to ~2 μm), interlaced, and seem to emerge from the microtubular structures. It should be noticed also the presence of some particles on the surface of the microtubes, embedded in the nanowire networks. We have already mentioned that other BN microtubes were obtained by our group 10 years ago by decomposition of continuous micrometric polymer fibers, but in contrast to the present microtubes they exhibited smooth surfaces.[24]

The crude sample was dispersed in ethanol by sonication. A droplet of this ethanol slurry was deposited on a holey carbon grid for TEM observation. As can be seen from the low-magnification TEM image of Figure 4, the microtube surfaces are made of graphitic sheets, agglomerated, and partially rolled on themselves, and are randomly distributed and oriented all along the microtube axis. Nanotubes of heterogeneous diameters are emerging from this agglomerate. The nanotube diameters are in the range 5−30 nm. HRTEM images revealed that these nanotubes are pure multiwalls of high crystalline quality, and nonbamboo-like nanostructures (Figure 5). To illustrate their wide distribution in diameter and then in number of walls, nanotubes with 3 and 13 graphitic layers are presented in Figure 5, panels a and b, respectively. In the HRTEM image of a multiwall nanotube (Figure 5a), as expected, graphitic layers are always oriented along the nanotube axis and separated by a distance of ~0,34 nm, characteristic of a d_{002} spacing in a hexagonal BN.[25] Planes perpendicular to the nanotube axis can also be observed. They are separated by a ~0.216 nm distance that corresponds to the (010) interplanar distance in *h*-BN (JCPDS card No. 34-0421). Compared to carbon NTs that do not show any preferential helicity and normally display a wide variety of chiralities, BN-layer stacking is atomically governed by a strong tendency, like grouped selective helical angles, leading to some unique structural features. In Figure 6a, vertical atomic columns (hexagonal BN stacking) are visible for the wall fringes and the corresponding diffraction pattern is characteristic of the so-called preferential zigzag tube layer orientation.[26] The nanotubes exhibit mainly close-ends and examples of these tips are presented in Figure 6b. It is also important to notice that few solid heaps are randomly attached to nanotube outer surfaces or seem occasionally even located inside the nanotubes (Figures 5 and 6).

Chemical analysis was performed by electron energy-loss spectroscopy during TEM investigations. Figure 7 shows the EELS spectrum recorded on a ~10 nm diameter nanotube similar to the one presented in Figure 5b confirming the formation of boron nitride nanotubes. The core-level electronic structure was examined by measuring the B1s and N1s excitation edges. The fine structures of B1s edges are represented in Figure 7a, inset. A comparison with corresponding fine structures from bulk *h*-BN shows that features are very similar with no significant shift in the peaks position, but their intensities are not identical.[27] The B1s spectrum of BN multiwall NTs exhibits a sharp peak at 193 eV (denoted a) due to the excitonic B1s→ π^* transition, which is only allowed for momentum transfers perpendicular to the BN sheet. The excitonic B1s → σ^* transition is represented by the peaks centered at 200, 206, and 216 eV and the shoulder at ~236 eV, denoted b, c, d, and e, respectively. This particular shape of the excitonic transition attests for a sp^2 type of bonding as in *h*-BN. A similar assignment not shown here can be made for the N−K edge spectrum. In agreement with Raman spectroscopy, the presence of traces of carbon in the crude sample is attested by the peak at 285 eV corresponding to the K-shell excitation of C. Even if the formation of homogeneous B−C−N or heterogeneous BN−C nanotubes cannot be completely excluded, the carbon-rich atmosphere used for the growth process together with the

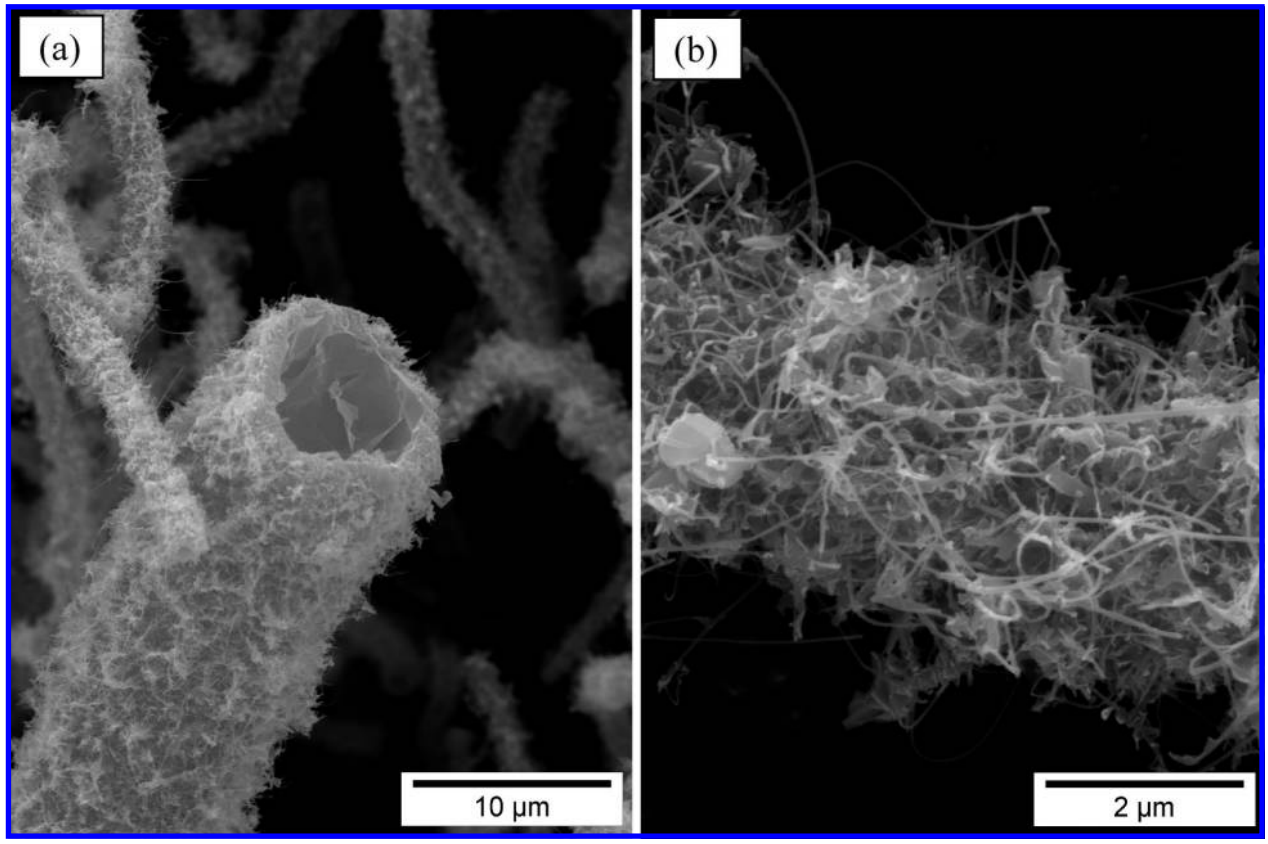

Figure 3. SEM images of the BN microtubes with heterogeneous diameters (a) which are entirely covered by very-long and interlaced nanotubes (b).

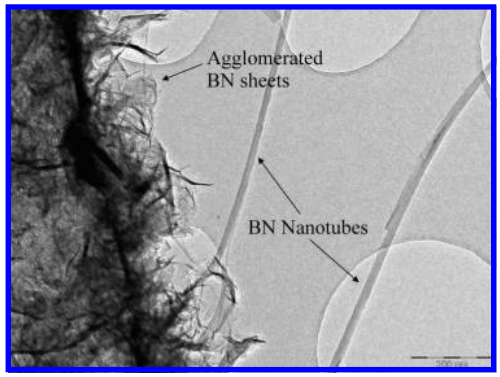

Figure 4. Low-magnification conventional TEM image of a BN microtube made of agglomerated BN sheets from which BN nanotubes are emerging.

observations of solid aggregates randomly stuck onto the nanotube surfaces support a carbon-surface pollution of BN nanotubes. The elucidation of this point is a crucial step toward applications since C-doped BN nanotubes were demonstrated to behave as good field emitters and semiconductors with a possible gap-tuning depending on carbon content.[28] To obtain more experimental evidence concerning chemical composition, line-scans have been performed during EELS experiments across several BN NTs. An example is shown on Figure 7b. This figure clearly shows that carbon content decreases from the surface to the core, inversely to boron and nitrogen contents. This result supports our assumption of carbon contamination localized on the surface of the BN NTs.

Growth Mechanism of BN Tubular Structures and Fabrication of Elegant BN Microflowers. ***Role of the Carbon Source (Polypropylene).*** To obtain some information about the growth mechanism, complementary experiments have been

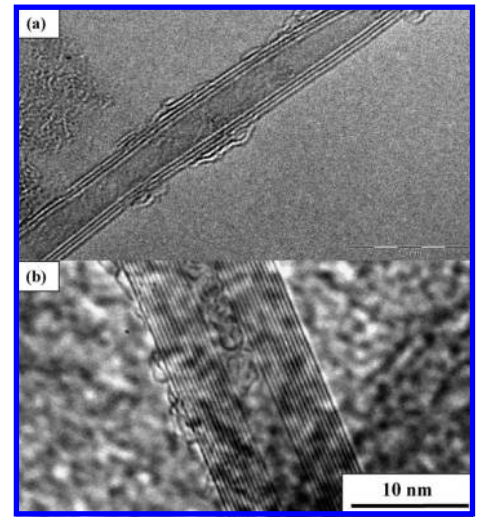

Figure 5. HRTEM images of a 3-wall BN nanotube (a) and of a 13-wall BN nanotube grown from the surface of the BN microtube.

performed with modifications of the experimental parameters. First of all, we have to discuss the role of the carbon precursors (polypropylene) used to grow the nanotubes. We have previously demonstrated elsewhere that the decomposition of polypropylene into volatile hydrocarbons permits the surface (nano)structuration of the graphite condensation plate, which favors the growth of 1D nanostructures, such as SiC nanowires, instead of the formation of a (2D) coating onto the substrate.[20] To confirm this effect, an experiment similar to the one depicted above but performed by omitting the carbon source (polypropylene) was undertaken. A white powdery coating was collected at the lower face of the graphite condensation plate. Raman analysis indicated

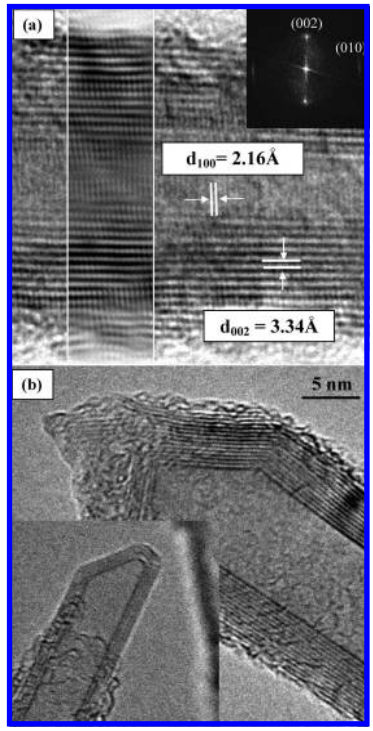

Figure 6. HRTEM image of a BN nanotube showing the (100) and the (002) interplanar distances of boron nitride (a) and examples of nanotube close-ends (b).

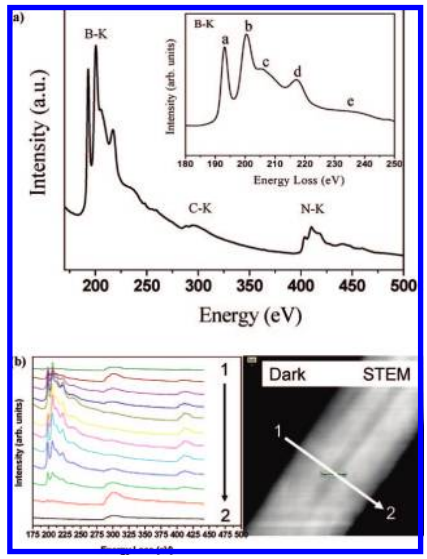

Figure 7. (a) EELS spectrum recorded on a ~10 nm diameter nanotube similar to the one presented in Figure 5b; the inset gives the fine structure of B1s. (b) On the left, EELS spectra, in line scan mode, and on the right the corresponding Dark STEM image, in line scan mode, of a BN NTs of the same diameter.

that this coating is composed of pure boron nitride without carbon pollution. This result, together with the difference of colors between the as-grown products obtained with and without polypropylene, gray or white, respectively, supports the carbon surface contamination of BN micro-/nanotubes, due to the cracking/condensation of carbon-based volatiles originating from polypropylene. SEM observations revealed that the coating is made of agglomerated BN sheets oriented preferentially perpendicular to the substrate surface (Figure 8a). This coating is decorated with elegant flower-like spherical shapes (white arrow, Figure 8a). The density of these BN flowers is variable and not

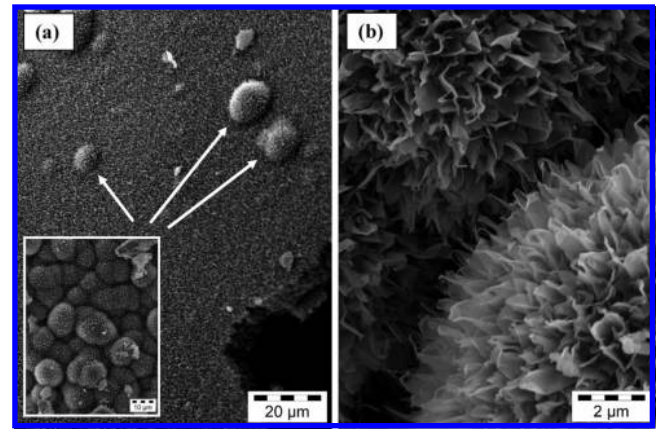

Figure 8. SEM images of the coating formed onto the lower face of the graphite condensation plate when the carbon source is omitted: BN sheets, roughly oriented perpendicular to the substrate, are obtained (a); this coating is decorated with BN flowers (a, white arrow), the flower density strongly varies along a substrate (inset a). BN flowers at higher magnification (b).

reproducible: it changes drastically depending on the observed region of the substrate and from one substrate to another one. As an illustration, the inset of the Figure 8a shows a region only constituted of BN flowers. Figure 8b shows a SEM image of the flower at higher magnification. The presence of these BN flowers together with their random distribution onto the coating are attributed to an imperfect polishing of the graphite substrate. In other words, we suggest that asperities on the surface of the graphite condensation plate lead to the formation of these flowers. These BN coatings and flowers remind us of the thorn-like BN nanostructures obtained by Jang et al. on the surface of SiC nanowires.[29] It is interesting to notice a common feature between Jang's works and the present study is that BN is formed under an ammonia atmosphere. Since BN is rather obtained as polycrystalline micrometric particles under nitrogen,[30] we can attribute the preferential formation of BN sheets to "substrate/solid (BN)/gaz (NH_3)" interactions during the growth. This assumption is in good agreement with the results described by Chen et al. concerning the influence of nitriding gases onto the growth of BN nanotubes.[31] These authors demonstrate that ammonia favors the 2D growth of BN by comparison to pure N_2 or N_2-H_2 mixture which favor a 3D growth. We can conclude from the comparison of the experiments performed with or without the carbon source that the surface nanostructuration of the substrate, as described above, plays a key role in the growth of BN tubular structures.

Role of the Boron Source and Suggested Growth Mechanism. The conversion of boron oxide into boron nitride by ammonia at 1500 °C (eq 1) via successive solid−gas reactions was demonstrated by Economy et al. during the preparation of micrometric BN fibers from boron oxide fibers.[32]

$$2NH_3(g) + B_2O_3(s) \rightarrow 2BN(s) + 3H_2O(g) \qquad (1)$$

According to Economy, the conversion mechanism of B_2O_3 by NH_3 involves the formation of polyboroxine intermediates. These polymers can be seen as the oxygen-based analogues of polyborazines,[33] with B_3O_3 rings linked through oxygen bridges. However, the transport of boron through the gas phase, and from the boat to the condensation plate, is attested by the formation of BN containing substances at the lower face of the substrate. We assume that the boron-based volatiles may be some boroxine derivatives, $R_3B_3O_3$ (with R = −OH or $-NH_2$), the oxygen-based analogues of the well-known borazine derivatives. We

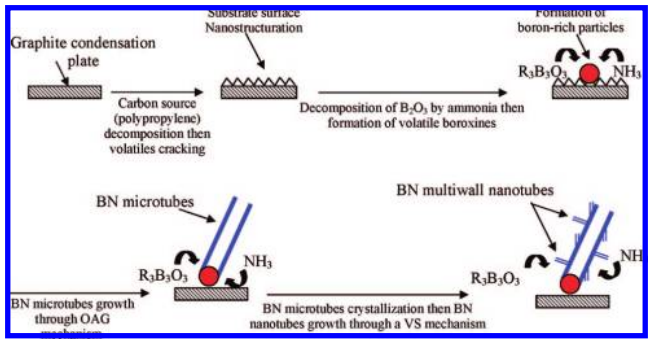

Figure 9. Suggested multistep mechanism for the growth of BN hierarchical tubular structures based on the OAG mechanism for the growth of BN microtubes followed by a VS mechanism for the growth of BN nanotubes.

suggest therefore the existence of a competition between volatilization and polymerization of the boroxines, in a similar way as can be observed with some borazine derivatives.[24] Attempts to characterize these derivatives by gas chromatography coupled with mass spectrometry were unsuccessful due to their extremely low concentration and high reactivity. It is therefore possible to envisage also the formation of $B_2O_2(g)$, even if the latter is preferentially formed by the direct solid-state reaction between $B_2O_3(s)$ and other oxides rather than ammonia.[15,20] The (weak) temperature gradient between the boat and the condensation plate is supposed to be the driving force for the transport of boron in the vapor phase. At higher temperatures, the precursors condensed onto the graphite substrate are converted into BN. We suggest thus the following multistep mechanism (Figure 9):

(1) The thermal decomposition of polypropylene from 150 °C yields a surface nanostructuration of the graphite condensation plate.

(2) At higher temperatures, and below 1000 °C according to Economy et al.,[32] ammonia decomposes boron oxide to give volatile precursors, presumably boroxine derivatives, which further condensate at the lower face of the condensation plate, due to a weak thermal gradient. Due to surface roughness of the substrate, micrometric particles, rich in boron, are formed.

(3) Due to continuous supplies of boron and nitrogen from the vapor phase, we suggest that the micrometric particles can allow the fabrication of BN microtubes via an oxide-assisted growth (OAG) mechanism. The latter has been first suggested by Lee et al. for the formation of Si nanowires from silicon-rich liquid micrometric particles.[34] This mechanism is in some way similar to the well-known Vapor−Liquid−Solid (VLS) mechanism, originally proposed by Wagner and Ellis for the formation of monocrystalline silicon microfibers/whiskers[35] and extended by Oberlin et al. to carbon tubular fibrous materials.[36] Due to the crystallographic similarities between carbon graphite and hexagonal boron nitride, the formation of boron nitride microtubes rather than full microfibers is not surprising. We have to mention also that the direct OAG growth of BN nanotubes was also reported by Ma et al. from a designed precursor $B_4N_3O_2H$.[14]

(4) At the highest temperature, crystallization of the BN microtubes occurs. Due to "solid (BN)/gas (NH_3)" interactions, this crystallization step initiates the formation of BN sheets and therefore of BN multiwall nanotubes. The growth of these BN sheets and nanotubes is fed by the vapor phase, which is rich in boron ($R_3B_3O_3$) and nitrogen (NH_3 or N_2 resulting from the partial decomposition of ammonia above 1000 °C). The mechanism is therefore related to a Vapor−Solid mechanism (ammonia/nitrogen/boroxine BN nanotubes) also called root-growth mechanism. The latter is presumably very likely similar to the one described by Chen et al. for the formation of BN nanotubes from annealing of ball-milled boron powders under ammonia.[31] This VS or root-growth mechanism is also in good agreement with the closed tips of the nanotubes, since a VLS mechanism would have led to spherical tips containing the starting nanoparticles or even to open-ends if these nanoparticles were separated from the NTs during the growth process.

Conclusions

BN tubular structures with hierarchical sizes have been prepared on a graphite condensation plate with a simple process based on cheap reagents. The nanostructuration of the substrate surface, achieved by in situ cracking of hydrocarbons, plays a key role in the formation of these tubular structures. The transportation of boron from the solid source to the substrate occurs presumably via boroxine derivatives. We suggested that BN microtubes have been formed by an OAG growth mechanism while BN nanotube formation occurred in a second step, at higher temperature, from a VS (root-growth) mechanism initiated by the surface crystallization of the BN microtubes. When the carbon source is omitted, a homogeneous coating made of BN sheets is formed perpendicular to the substrate surface. This coating is randomly decorated with elegant BN flowers, which presumably result from asperities at the surface of the substrate. This BN coating can find valuable applications for tuning the wetting properties of substrates. The as-grown BN nanotubes, which can be separated from the microtubes by high-power sonication, are featured by high length, good crystalline quality (compared to bamboo-like NTs), one close tip, and diameters in the range 5−30 nm. The present process, which allows the large-scale fabrication of BN NTs from cheap reagents and equipments, would open new perspectives toward BN NTs properties investigation and BN NTs applications. The fabrication of BN micrometric fibrous materials covered by BN nanotubes opens new perspectives in (nano)composite materials, BN NTs acting as nanoanchors to enhance the matrice-to-fibers bonding.

Acknowledgment. We gratefully acknowledge the Common Center for Optical Microspectrometry (CECOMO) for Raman spectroscopy support, the Technological Center of Microstructures (CTμ) of the University Lyon 1, and the Laboratory of Condensed Matter Physics and Nanostructures (Laboratoire de Physique de la Matière Condensée et Nanostructures, LPMCN) for access to SEM and TEM, respectively.

References and Notes

(1) Chopra, N. G.; Zettl, A. *Solid State Commun.* **1998**, *105*, 297.
(2) Blase, X.; Rubio, A.; Louie, S. G.; Cohen, M. L. *Europhys. Lett.* **1994**, *28*, 335.
(3) Chopra, N. G.; Luyken, R. J.; Cherrey, K.; Crespi, V. H.; Cohen, M. L.; Louie, S. G.; Zettl, A. *Science* **1995**, *269*, 966.
(4) (a) Loiseau, A.; Willaime, F.; Demoncy, N.; Hug, G.; Pascard, H. *Phys. Rev. Lett.* **1996**, *76*, 4737. (b) Terrones, M.; Hsu, W. K.; Terrones, H.; Zhang, J. P.; Ramos, S.; Hare, J. P.; Castillo, R.; Prassides, K.; Cheetham, A. K.; Kroto, H. W.; Walton, D. R. M. *Chem. Phys. Lett.* **1996**, *259*, 568.
(5) Lee, R. S.; Gavillet, J.; Lamy de la Chapelle, M. L.; Loiseau, A.; Cochon, J. L.; Pigache, D.; Thibault, J.; Willaime, F. *Phys. Rev. B* **2001**, *64*, 121405.
(6) Shimizu, Y.; Moriyoshi, Y.; Tanaka, H.; Komatsu, S. *Appl. Phys. Lett.* **1999**, *75*, 929.
(7) Bartnitskaya, T. S.; Oleinik, G. S.; Pokropivnyi, A. V.; Pokropivnyi, V. V. *JETP Lett.* **1999**, *69*, 163.
(8) Gan, Z. W.; Ding, X. X.; Huang, Z. X.; Huang, X. T.; Cheng, C.; Tang, C.; Qi, S. R. *Appl. Phys. A: Mater. Sci. Process.* **2005**, *81*, 527.

(9) Xu, L.; Peng, Y.; Meng, Z.; Yu, W.; Zhang, S.; Liu, X.; Qian, Y. *Chem. Mater.* **2003**, *15*, 2675.
(10) Golberg, D.; Bando, Y.; Han, W.; Kurashima, K.; Sato, T. *Chem. Phys. Lett.* **1999**, *308*, 337.
(11) Chen, Y.; Fitz Gerald, J.; Williams, J. S.; Bulcock, S. *Chem. Phys. Lett.* **1999**, *299*, 260.
(12) Velazquez-Salazar, J. J.; Munoz-Sandoval, E.; Romo-Herrera, J. M.; Lupo, F.; Rühle, M.; Terrones, H.; Terrones, M. *Chem. Phys. Lett.* **2005**, *416*, 342.
(13) Lourie, O. R.; Jones, C. R.; Bartlett, B. M.; Gibbons, P. C.; Ruoff, R. S.; Buhro, W. E. *Chem. Mater.* **2000**, *12*, 1808.
(14) Ma, R.; Bando, Y.; Sato, T. *Chem. Mater.* **2001**, *13*, 2965.
(15) Tang, C. C.; Bando, Y.; Sato, T.; Kurashima, K. *Chem. Commun.* **2002**, 1290.
(16) Zhi, C. Y.; Bando, Y.; Tang, C. C.; Golberg, D. *Solid State Commun.* **2005**, *135*, 67.
(17) Bechelany, M.; Bernard, S.; Brioude, A.; Cornu, D.; Stadelmann, P.; Charcosset, C.; Fiaty, K.; Miele, P. *J. Phys. Chem. C* **2007**, *111*, 13378.
(18) Golberg, D.; Bando, Y.; Tang, C. C.; Zhi, C. Y. *Adv. Mater.* **2007**, *19*, 2413.
(19) Terrones, M.; Romo-Herrera, J. M.; Cruz-Silva, E.; López-Urías, F.; Muñoz-Sandoval, E.; Velázquez-Salazar, J. J.; Terrones, H.; Bando, Y.; Golberg, D. *Mater. Today* **2007**, *10*, 30.
(20) Bechelany, M.; Brioude, A.; Stadelmann, P.; Ferro, G.; Cornu, D.; Miele, P. *Adv. Funct. Mater.* **2007**, *17*, 3251.
(21) Nemanich, R. J.; Solin, S. A.; Martin, R. M. *Phys. Rev. B* **1981**, *23*, 6348.
(22) Choi, H. C.; Bae, S. Y.; Jang, W. S.; Park, J.; Song, H. J.; Shin, H. J. *J. Phys. Chem. B* **2005**, *109*, 7007.
(23) Eklund, P. C.; Holden, J. M.; Jishi, R. A. *Carbon* **1995**, *33*, 959.
(24) Cornu, D.; Miele, P.; Faure, R.; Bonnetot, B.; Mongeot, H.; Bouix, J. *J. Mater. Chem.* **1999**, *9*, 757.
(25) *Synthesis and Properties of Boron Nitride, Materials Science Forum*; Pouch, J. J., Alterovitz, S. A., Eds.; Trans Tech Publications: Zürich, Switzerland, 1990; pp54−55.
(26) Zhang, X. F.; Zhang, X. B.; Van Tendeloo, G.; Amelinckx, S.; Op de Beeck, M. *J. Cryst. Growth* **1993**, *130*, 368.
(27) Loiseau, A.; Willaime, F.; Demoncy, N.; Hug, G.; Pascard, H. *Phys. Rev. Lett.* **1996**, *76*, 4737.
(28) (a) Golberg, D.; Dorozhkin, P. S.; Bando, Y.; Dong, Z.-C.; Tang, C. C.; Uemura, Y.; Grobert, N.; Reyes-Reyes, M.; Terrones, H.; Terrones, M. *Appl. Phys. A: Mater. Sci. Process.* **2003**, *76*, 499. (b) Golberg, D.; Dorozhkin, P.; Bando, Y.; Dong, Z.-C. *MRS Bull.* **2004**, *29*, 38.
(29) Jang, W. S.; Bae, S. Y.; Park, J.; Ahn, J. P. *Solid State Commun.* **2005**, *133*, 139.
(30) Hubacek, M.; Ueki, M.; Sato, T.; Broiek, V. *Thermochim. Acta* **1996**, *282−283*, 359.
(31) Yu, J.; Li, B. C. P.; Zou, J.; Chen, Y. *J. Mater. Sci.* **2007**, *42*, 4025.
(32) Economy, J.; Anderson, R. V.; Matkovich, V. I. *Appl. Polym. Symp.* **1969**, 377.
(33) Cornu, D.; Bernard, S.; Duperrier, S.; Toury, B.; Miele, P. *J. Eur. Ceram. Soc.* **2005**, *25*, 111.
(34) (a) Lee, S. T.; Wang, N.; Zhang, Y Y. F.; Tang, H. *MRS Bull.* **1999**, *24*, 36. (b) Wang, N.; Tang, Y. H.; Zhang, Y. F.; Lee, C. S.; Lee, S. T. *Phys. Rev. B* **1998**, *58*, R16024.
(35) Wagner, R. S.; Ellis, W. C. *Appl. Phys. Lett.* **1964**, *4*, 89.
(36) Oberlin, A.; Endo, M.; Koyama, T. *J. Cryst. Growth* **1976**, *32*, 335.

JP804286X